IEEE Access
Multidisciplinary | Rapid Review | Open Access Journal

Received April 28, 2021, accepted May 31, 2021, date of publication June 4, 2021, date of current version June 15, 2021.

Digital Object Identifier 10.1109/ACCESS.2021.3086477

A Thermal Infrared Land Surface Temperature Retrieval Algorithm for Thin Cirrus Skies Using Cirrus Optical Properties

XIWEI FAN[1,2], GAOZHONG NIE[1,2], YAOHUI LIU[3], AND LI NI[4]

[1]Key Laboratory of Seismic and Volcanic Hazards, China Earthquake Administration, Beijing 100029, China
[2]Institute of Geology, China Earthquake Administration, Beijing 100029, China
[3]School of Surveying and Geo-Informatics, Shandong Jianzhu University, Jinan 250101, China
[4]Key Laboratory of Digital Earth Science, Aerospace Information Research Institute, Chinese Academy of Sciences, Beijing 100094, China

Corresponding authors: Li Ni (nili@aircas.ac.cn) and Yaohui Liu (liuyaohui20@sdjzu.edu.cn)

This work was supported in part by the National Natural Science Foundation of China under Grant 42071337 and Grant 41601390, in part by the National Key Research and Development Program of China under Grant 2018YFC1504403 and Grant 2018YFC1504503, and in part by the Director Fund of Institute of Geology, China Earthquake Administration under Grant IGCEA2106.

ABSTRACT To acquire daytime land surface temperature (LST) in thin cirrus cloudy skies, we have developed a three-channel LST retrieval algorithm based on a widely used two-channel LST retrieval algorithm for the clear-sky conditions. In this algorithm, the LST is expressed as a multiple linear function of MODIS channels 29, 31 and 32 with the coefficients of the linear function dependent on the cirrus optical depth (COD) and cirrus effective radius (R). The influences from land surface emissivities (LSEs) are also considered in this algorithm. The simulated dataset shows that the LST could be estimated using the proposed algorithm with the root mean squire error (RMSE) less than 2.2 K in thin cirrus cloudy skies (COD less than 0.7) when viewing zenith angle (VZA) equivalent to 0°. As VZA is equivalent to 60°, the maximum RMSE are 2.7 K. The widely used generalized split-window (GSW) algorithm proposed for clear-sky conditions are used in cirrus cloudy skies, and the RMSEs of GSW algorithm estimated LST are 16.89 K and 22.32 K for VZA = 0° and VZA = 60° respectively when COD is 0.7. It indicates that the proposed three-channel algorithm can significantly improve the LST retrieval accuracy using thermal infrared data in cirrus cloudy skies. To estimate the LST errors caused by the uncertainties of COD, R, LSE and instrument noise, a sensitivity analysis was performed. It shows that the accuracy of cirrus COD is more important for the retrieval of LST compared with other parameters. The maximum total LST errors, taking into account all the input parameters' uncertainty and algorithm error itself, are 3.8 K and 4.3 K when VZA = 0° and VZA = 60° respectively.

INDEX TERMS Land surface temperature, thermal infrared remote sensing, retrieval algorithm, thin cirrus clouds, MODIS.

I. INTRODUCTION

Land surface temperature (LST) is a key parameter in the physics of land surface processes because it is involved in the energy balance as well as in the evapotranspiration and desertification processes [1], [2]. Satellite remote sensing offers the only possibility to measure LST over extended regions with high temporal and spatial resolution [3]. However, up to now, the traditional LST retrieval algorithms such as split-window [4] or single-channel algorithms [5] are dependent on clear-sky conditions. The atmospheres covered with clouds are usually masked for LST retrieval algorithm.

Cirrus clouds, with obvious low temperature compared with land surface [6], can significantly reduce the brightness temperate observed by satellite [7] and induce large errors on satellite thermal infrared (TIR) data retrieved LST. To reduce the influence of cirrus on LST retrieval, some algorithms are proposed [8], [9]. For example, Fan *et al.* [10] proposed a physically based night-time three-channel LST retrieval algorithm using MODIS Mid-infrared channel 20 and TIR channels 31 and 32. And considering the MODIS 1.39 μm channel is sensitive to cirrus, this channel is commonly used

The associate editor coordinating the review of this manuscript and approving it for publication was Geng-Ming Jiang.

to estimate cirrus reflectance and optical depth, as cirrus cloud commonly located at high altitude with the influence of water vapor above cirrus can be ignored reasonably. Taking the cirrus reflectance produces as input, the cirrus optical depth (COD) is acquired with a look up table method. Then, the day-time TIR LST retrieval errors induced by cirrus is reduced based on COD [11]. Note that, besides COD, cirrus clouds have a varied effective radius (R) [12] which changed from 0 to approximately 120 μm. Considering that besides COD, more cloud parameters such as cloud radius is available in most satellite cloud products, this study try to make use of cloud parameters of COD and R to improve LST retrieval accuracy under cirrus skies.

Considering the Moderate-Resolution Imaging Spectroradiometer (MODIS) has a complete set of cloud products and is widely used for LST retrieval with a retrieval accuracy of 1 K under clear-sky conditions [13], this study try to develop a LST retrieval algorithm for MODIS in thin cirrus cloudy conditions. Because of the cloud effective radius are available during daytime, this paper focuses on daytime LST retrieval. This paper is organized as follows: Section II gives the data used in this study; Sections III describes the methodology for the retrieval of LST; the results and some analysis are also given in Section IV; the sensitivity analysis is provided in Section V; Conclusions are presented in the last section.

II. DATA

In this study the atmospheric radiative transfer model MODerate resolution atmospheric TRANsmission (MODTRAN) [14] is used to simulate the MODIS data in thin cirrus cloudy skies for methodology development. As inputs of MODTRAN, 50 atmospheric profiles of Thermodynamic Initial Guess Retrieval (TIGR) database constructed by the Laboratoire de Meteorologie Dynamique (LMD) [15], [16], 54 land surface emissivities (LSEs) [17] of Advanced Spaceborne Thermal Emission Reflection Radiometer (ASTER) spectral library, and cirrus optical properties of Ice Cloud Bulk Scattering Models (http://www.ssec.wisc.edu/ice_models/) provided by Space Science and Engineering Center (SSEC) [18]–[20] are prepared. The 50 clear-sky atmospheric profiles with water vapor content (WVC) less than 5.0 g/cm^2 are selected from TIGR. Two types of simulated top of the atmosphere (TOA) brightness temperatures dataset in MODIS channels 29, 31, and 32 are established: one does not include the influences of thin cirrus clouds (Dataset-1) and one that does include such influences (Dataset-2). For Dataset-2, three cirrus top height (CTH) of 8 km, 12 km, and 16 km are used; and COD changes from 0.07 to 0.7 with a step of 0.07; and R changes from 5 μm to 60 μm in steps of 5 μm. To simulate different satellite viewing conditions, six different viewing zenith angles (VZAs) with VZA = 0°, 33.56°, 44.42°, 51.32°, 56.25° and 60° (Secant(VZA) = 1.0, 1.2, 1.4, 1.6, 1.8 and 2.0) are used in the simulations. The detail of simulate data production can refer to our previous work [11].

III. METHODOLOGY

Many split-window [21] or two-channel [22] algorithms were proposed to estimate LST in clear-sky conditions. Assuming the two-channel algorithms can also be used to estimate LST using the data measured at the base of thin cirrus clouds, the three-channel LST retrieval algorithm is proposed with combing a couple of two-channel algorithms in three different channels.

A. RADIATIVE TRANSFER EQUATION

Cirrus clouds are located generally at an altitude above 7 km in the mid-latitude and 9 km in the tropical region [23]. The low- and middle-level water clouds, major aerosol loadings, and 90-99% of the atmospheric water vapor are located below cirrus. As a consequence, the outgoing radiance at the top of the atmosphere (TOA) under clear-sky conditions is equal to the upward incoming radiance at cirrus base. This is a reasonable approximation for the channels situated in the thermal infrared window region where most radiation is coming from the lower atmosphere [24]. Thus, the TOA channel radiance in the satellite direction is:

$$I_i(\theta) = (1-N)\, I_i^{base}(\theta) + N \begin{bmatrix} I_i^{base}(\theta)\, t_i^d(\theta) + \\ \int_0^{\pi/2} I_i^{base}(\theta')\, t_i^s(\theta', \theta) \sin\theta' d\theta' + B_i(T_c)\, \varepsilon_i^c(\theta) \end{bmatrix} \quad (1)$$

In this expression, i is the channel number; N is the fractional cloud cover; $t_i^d(\theta)$ and $t_i^s(\theta', \theta)$ are the cloud direct and scattering transmittance in satellite direction for radiation incident $I_i^{base}(\theta)$ and $I_i^{base}(\theta')$ at cloud base in direction θ and θ' respectively; B_i is the Planck function weighted in channel i. Assuming that the cirrus cloud layer is isothermal, the cirrus radiation in the satellite direction can be taken as the radiance emitted by an temperature T_c with an emissivity of $\varepsilon_i^c(\theta)$.

To simplify, the incoming radiance at cirrus base is assumed to be isotropic. Thus the diffused transmittance in the satellite direction is defined as:

$$\overline{t_i^s}(\theta) = \int_0^{\pi/2} t_i^s(\theta', \theta) \sin\theta' d\theta' \quad (2)$$

Similarly, the cirrus directional reflectance at cirrus top $\overline{r_i}(\theta)$ can be defined in the same way; thus based on the Kirchoff's law the cirrus emissivity can be expressed as:

$$\varepsilon_i^c(\theta) = 1 - t_i^d(\theta) - \overline{t_i^s}(\theta) - \overline{r_i}(\theta) \quad (3)$$

With $I_i^{base}(\theta)$ expressed as $B_i(T_i^0)$, $I_i(\theta)$ expressed as $B_i(T_i)$, and eliminate the angular note, Eq. (1) can be expressed as:

$$B_i(T_i) = (1-N)\, B_i\left(T_i^0\right) + N \begin{bmatrix} B_i\left(T_i^0\right)\left(t_i^d + \overline{t_i^s}\right) \\ +B_i(T_c)\left(1 - t_i^d - \overline{t_i^s} - \overline{r_i}\right) \end{bmatrix} \quad (4)$$

Because of the strong forward scattering effect, the cirrus reflectance is relatively small. Taking the six default atmospheric profiles in MODTRAN for example, the $\overline{r_i}$ of MODIS

channels 29, 31 and 32 are less than 0.01 for t_{32}^d equivalent to 0.5 and R changes from 20 μm to 60 μm when CTH is 10 km and cirrus thickness is 1 km; the elimination of $\overline{r_i}$ in Eq.(4) cause T_c decrease less than 0.59 K, 0.93 and 0.87 K (averagely 0.21 K, 0.32 K and 0.29 K) for channels 29, 31 and 32, respectively. But the decreasement of T_c can be greater than 1 K for the atmospheric profiles with low WVC such as mid-latitude winter and sub-arctic winter when R is less than 20 μm, because of the relatively strong back scattering effect as R decrease.

After eliminate $\overline{r_i}$, to obtain an algorithm involving temperatures rather than radiances, the first-order Taylor series expansion of the Planck function $B_i(T)$ around T_i^0 is used in Eq.(4). That is,

$$B_i(T) = B_i\left(T_i^0\right) + \left(T - T_i^0\right)\frac{\partial B_i\left(T_i^0\right)}{\partial T} \quad (T = T_i \text{ or } T_c) \tag{5}$$

Sobrino *et al.* [25] pointed out that in the 10.5-12.5 μm and for moderate temperature departures $\left|T - T_i^0\right| \leq 10 - 15$ K, Eq.(5) is accurate to better than 1 percent. But considering the cirrus clouds temperature T_c is significantly cooler than T_i^0, T_c generally cooler than $-41°$ [26], the errors in the approximation of Planck function need to take into account. Thus, from Eq.(4) and Eq.(5) we can get:

$$T_i = \left[1 - N\left(1 - \tau_i\right)\right]T_i^0 + N\left(1 - \tau_i\right)T_c + \Delta T_i, \tag{6}$$

where ΔT_i is the total errors caused by the approximation of $B_i(T_c)$ and $B_i(T_i)$ in Eq.(4) and $\tau_i = t_i^d + \overline{t_i^s}$.

Figure 1 presents the relationship between ΔT_i ($i = 29$, 31 or 32) versus $T_c - T_i^0(-110 \text{ K} \leq T_c - T_i' \leq -30 \text{ K})$, when τ_i is 0.5, N is equivalent to 1, T_c increases from 210 K to 270 K and T_i^0 increases from 270 K to 320 K both in steps of 1 K. It indicates ΔT_i can be expressed as a linear function of $T_c - T_i^0$ with most of the RMSEs between the linearly estimated ΔT_i and the actual values of ΔT_i less than 1 K as the red symbols show. Because ΔT_i is also dependent on τ_i and N, ΔT_i is finally expressed as:

$$\Delta T_i = c_i N^2\left(1 - \tau_i\right)^2\left(T_c - T_i^0\right) + d_i N\left(1 - \tau_i\right)\left(T_c - T_i^0\right) + f_i N\left(1 - \tau_i\right)\left(N\left(1 - \tau_i\right) \leq 0.5\right) \tag{7}$$

where c_i, d_i and f_i are the regression coefficients. To determine those three coefficients, the ΔT_i is calculated according Eq.(6) with $N\left(1 - \tau_i^c\right)$ changes from 0.01 to 0.5 in step of 0.01, T_c increases from 210 K to 270 K and T_i^0 from 270 K to 320 K both in step of 1 K. Then c_i, d_i and f_i ($i = 29$, 31 and 32) are determined using Levenberg-Marquardt method. The values of the coefficients and the RMSEs between actual ΔT_i and the estimated values using Eq.(7) are given in Table 1.

B. THE THREE CHANNEL ALGORITHM

Sobrino and Raissouni [22] proposed a two-channel algorithm with separate terms for the atmospheric and land surface emissivity corrections to retrieve LST from

TABLE 1. The coefficients and RMSEs for the estimate of ΔT_i based on eq.(7) in channels 29, 31 and 32.

Channel	c_i	d_i	f_i (K)	Total RMSE (K)
29	0.25	-0.60	-13.29	0.49
31	0.22	-0.46	-10.37	0.41
32	0.20	-0.41	-9.36	0.38

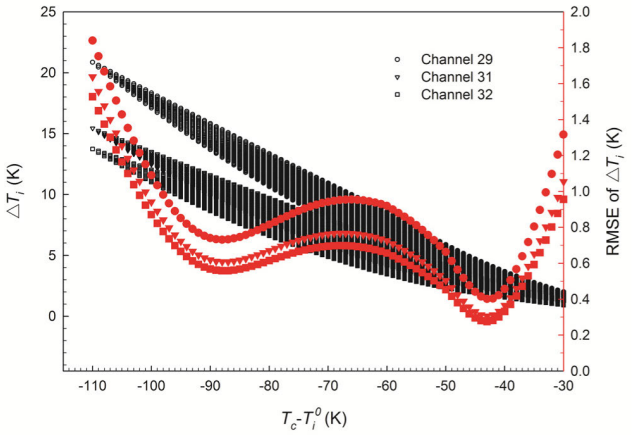

FIGURE 1. Temperature errors ΔT_i caused by the approximation of Planck function for channels 29, 31 and 32 in Eq. (6). The τ_i ($i = 29$, 31 or 32) is 0.5, N is equivalent to 1, T_c increases from 210 K to 270 K and T_i^0 increases from 270 K to 320 K both in steps of 1 K. The RMSEs between actual ΔT_i and the estimated values versus $T_c - T_i^0$ are shown in red symbols.

NOAA-AVHRR data. It can be written as:

$$T_s = T_i + a_1\left(T_i - T_j\right) + a_2\left(1 - \varepsilon\right) + a_3 W\left(1 - \varepsilon\right) + a_4\Delta\varepsilon + a_5 W\Delta\varepsilon + a_0 \tag{8}$$

where, T_s is LST, T_i and T_j are the TOA brightness temperatures in channels i and j, ε is the mean channel emissivity $\varepsilon = (\varepsilon_i + \varepsilon_j)/2$, $\Delta\varepsilon$ is the emissivity difference $\Delta\varepsilon = \varepsilon_i - \varepsilon_j$, W is the total atmospheric WVC and $a_i (i = 0 - 5)$ is the numerical coefficient of the two-channel algorithm.

In cirrus cloudy skies, the radiation at cirrus base $B_i\left(T_i^0\right)$ need to take into account the cirrus downward radiation reflected by ground and downward spherical albedo compared with clear-sky conditions, assuming that the atmospheric water vapor above the height of cirrus clouds is ignored. Similarly, taking six default atmospheric profiles in MODTRAN for example, when CTH is 10 km, COD (12 μm) 0.7, cirrus thickness 1 km and R varies from 5 to 60 μm, ignoring the cirrus downward radiation and spherical albedo effect in $B_i\left(T_i^0\right)$ can cause T_i^0 reduce averagely 0.45 K, 0.22 K and 0.24 K (maximum 0.82 K, 0.41 K and 0.56 K) for channels 29, 31 and 32, when LSEs are 0.8, 0.9 and 0.9 respectively. It indicates that T_i^0 can be simplified as the corresponding value in clear-sky conditions without losing much accuracy. In other words, the Eq.(8) can be employed to estimate LST in cirrus cloudy skies with the brightness temperatures measured at cirrus cloud base.

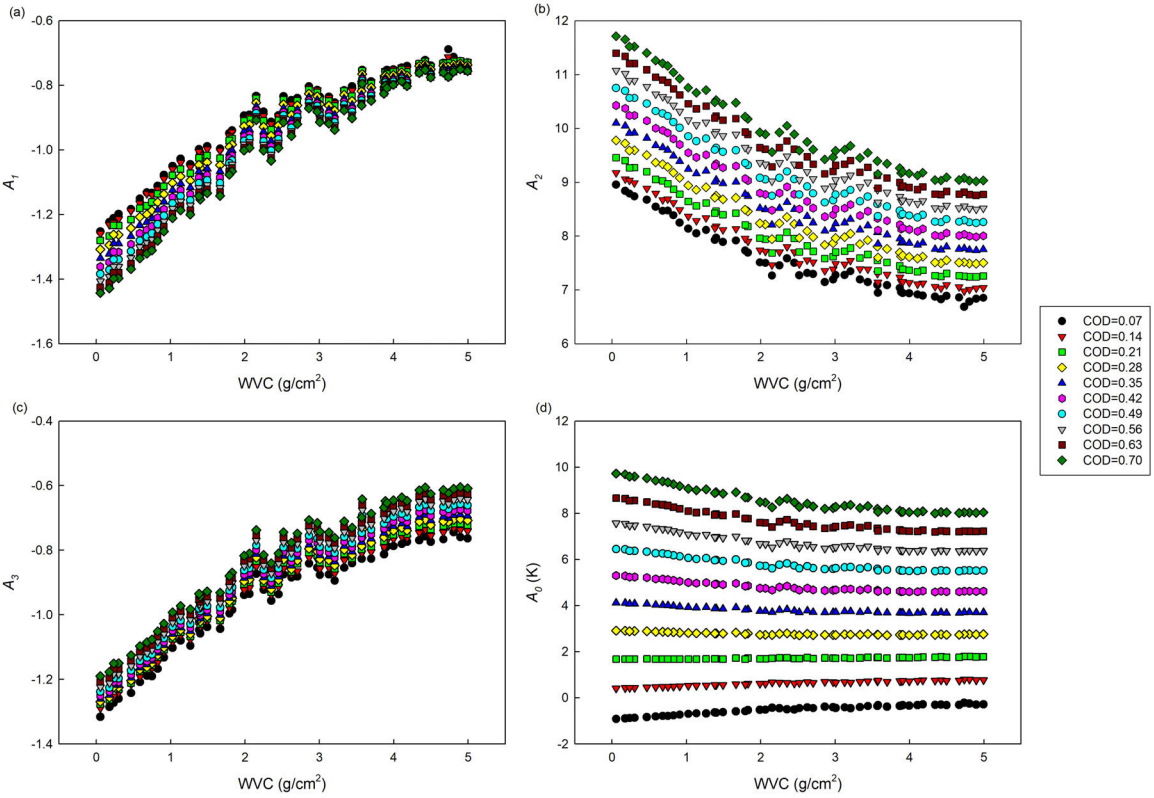

FIGURE 2. The three-channel LST retrieval algorithm coefficients A_1, A_2, A_3 and A_0 versus atmospheric WVC for different CODs when R equivalent to 60 μm. (a) for A_1, (b) for A_2, (c) for A_3 and (d) for A_0, respectively.

To retrieval LST in cirrus cloudy skies, a couple of two-channel algorithms in channels i, j and k are used:

$$\begin{cases} T_s = T_i^0 + a_1\left(T_i^0 - T_j^0\right) + a_2\left(1-\varepsilon_1\right) \\ \qquad + a_3 W\left(1-\varepsilon_1\right) + a_4\Delta\varepsilon_1 + a_5 W\Delta\varepsilon_1 + a_0 \\ T_s = T_i^0 + b_1\left(T_i^0 - T_k^0\right) + b_2\left(1-\varepsilon_2\right) \\ \qquad + b_3 W\left(1-\varepsilon_2\right) + b_4\Delta\varepsilon_2 + b_5 W\Delta\varepsilon_2 + b_0 \end{cases} \tag{9}$$

where T_i^0, T_j^0 and T_k^0 are the brightness temperatures in channels i, j and k measured at the cirrus base, ε_1, $\Delta\varepsilon_1$, ε_2 and $\Delta\varepsilon_2$ are the mean and difference of corresponding channel emissivities, a_i and $b_i(i = 0-5)$ are the numerical coefficients of the two-channel algorithm. Inserting Eq.(6) and Eq.(7) into Eq.(9) and eliminating T_c in both equations of Eq.(9) yields:

$$\begin{aligned} T_s = {} & T_i + A_1\left(T_i - T_j\right) + A_2\left(T_i - T_k\right) \\ & + \left[a_2\left(1-\varepsilon_1\right) + a_3 W\left(1-\varepsilon_1\right) + a_4\Delta\varepsilon_1 + a_5 W\Delta\varepsilon_1\right] \\ & + A_3\left[b_2\left(1-\varepsilon_2\right) + b_3 W\left(1-\varepsilon_2\right) + b_4\Delta\varepsilon_2 + b_5 W\Delta\varepsilon_2\right] \\ & A_4 + A_0 \end{aligned} \tag{10}$$

in which, the definition of A_1, A_2, A_3, A_4 and A_0 can be find in our previous work [11].

From the theoretical formulations of Eq.(10), the cirrus clouds dependent coefficients A_1, A_2, A_3, A_4 and A_0 can be studied. To do this, the coefficients a_n and $b_n(n = 0-5)$ in Eq. (9), as well as τ_i, τ_j and τ_k are calculated firstly by simulated data. With the LSTs and corresponding TOA brightness temperatures in Dataset-1 when VZA $= 0°$, the coefficients are determined using the statistical regression method as $i = 31$, $j = 29$ and $k = 32$. The coefficients a_n, $b_n(n = 0-5)$ and RMSEs between the LSTs set in MODTRAN and the corresponding values estimated using Eq.(9) are shown in Table 2.

Besides that, the cirrus transmittances τ_{29}, τ_{31} and τ_{32} are obtained using the selected atmospheric profiles from TIGR when cirrus CTH is equivalent to 10 km with a thickness of 1 km and R is 60 μm. To study the variations of A_1, A_2, A_3, A_4 and A_0 with cirrus microphysical properties, the *COD* (12 μm) changes from 0.07 to 0.7 in steps of 0.07. Together with the values of a_n and b_n in Table 2, the A_1, A_2, A_3 and A_0 are calculated based on Eq.(14) and Eq.(15) in [11] and are given in Figure 2.

Figure 2 indicates that A_1, A_2, A_3 and A_0 change almost linearly with COD for a given WVC. Except COD, those four coefficients are also affected by the atmospheric WVC. This is because the remnant a small amount of atmospheric water vapor above cirrus cloud, what is ignored in this study. Besides COD, to study the influences of R, the A_1, A_2, A_3 and A_0 with COD (12 μm) fixed to 0.7 and R changes from 5 μm to 60 μm in steps of 5 μm are given in Figure 3. It shows that A_1, A_2, A_3 and A_0 are also dependent on R. In addition, the values of A_1, A_2, A_3 and A_0 when R is less than 20 μm are

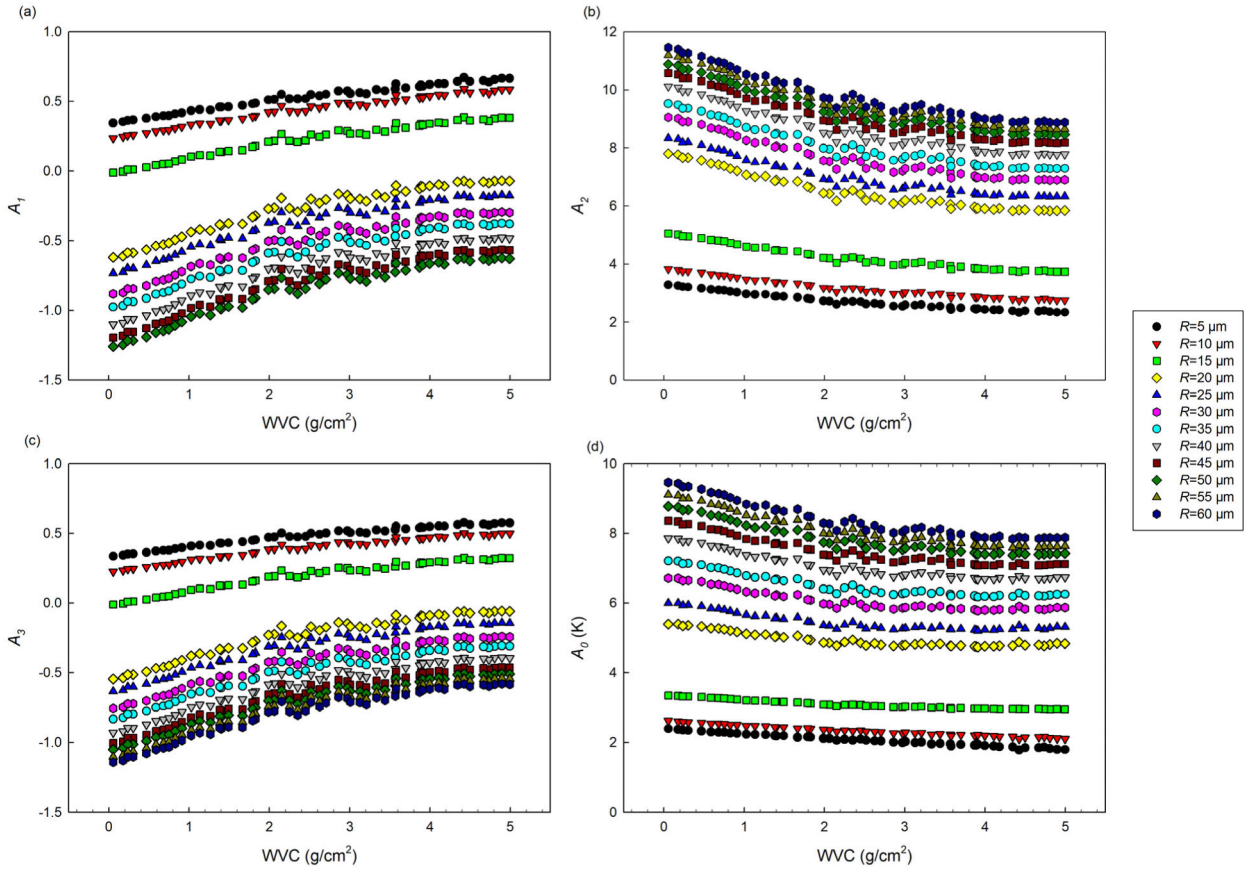

FIGURE 3. Relationships between A_1, A_2, A_3 and A_0 versus atmospheric WVC for different R with COD equivalent to 0.7. (a) for A_1, (b) for A_2, (c) for A_3 and (d) for A_0, respectively.

TABLE 2. Values of two-channel LST retrieval algorithm coefficients in eq.(9).

Coefficients	n=1	n=2	n=3	n=4	n=5	n=0	RMSE (K)
a_n	0.9	-23.9	25.9	-30.8	-5.5	1.5	2.5
b_n	3.7	67.0	-8.6	-238.9	40.4	-0.1	0.6

distinguished from the values when R is larger than 20 μm, because the cirrus clouds optical properties are significantly different as R is less than 20 μm. So that, the proposed daytime LST retrieval algorithm needed to divide into two parts according to R.

Considering the relatively small contributions of W for the accuracy of LST retrieval using Eq.(9) and that the A_3 and A_4 are close to 0, the W in Eq.(10) is eliminated and a three-channel algorithm for the estimate of LST in daytime cirrus cloudy skies is proposed:

$$\begin{aligned} T_s = {} & T_{31} + \left(w_1 + w_2 * COD + w_3 p * R\right)\left(T_{31} - T_{29}\right) \\ & + \left(w_4 + w_5 * COD + w_6 * R\right)\left(T_{31} - T_{32}\right) \\ & + w_7 \Delta\varepsilon_1 + w_8\left(1 - \varepsilon_1\right) + w_9 \Delta\varepsilon_2 + w_{10} * COD \\ & + w_{11} * R + w_0 \end{aligned} \tag{11}$$

where T_{29}, T_{31} and T_{32} are the TOA brightness temperatures in channels 29, 31 and 32; COD and R are cirrus optical depth and effective radius, respectively; ε_1 and $\Delta\varepsilon_1$ are the LSE mean and difference respectively in channels 29 and 31; $\Delta\varepsilon_2$ is the LSE difference in channels 31 and 32; w_n $(n = 0 - 11)$ is the regression coefficients depending on the viewing zenith angles. Because of the particularity of cirrus effective radius discussed above, this algorithm is divided into two groups respect to R, that is $R \geq 20$ μm and R < 20 μm. Because of the length of this paper, the conditions with R less than 20 μm are not discussed.

IV. RESULTS

A. RETRIEVAL ACCURACY

To evaluate the performance of the proposed daytime three-channel LST retrieval algorithm in thin cirrus cloudy conditions, the simulated Datset-2 are used. Then the coefficients w_n $(n = 0 - 11)$ in Eq.(11) are determined with statistical regression method. Figure 4 shows the procedure for acquiring the coefficients of Eq.(11).

Figure 5 shows the RMSEs between actual LSTs and LST values estimated using Eq.(11) versus COD for different VZAs in daytime. It shows that the RMSEs increase with the increasement of COD, vary from 1.3 K to 2.2 K for R greater than 20 μm in vertical view conditions. The accuracy

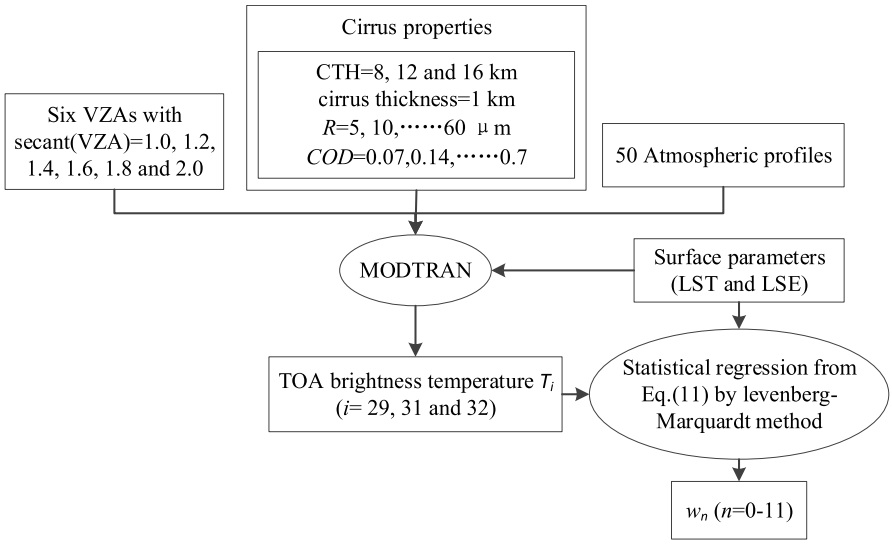

FIGURE 4. Procedure for acquiring coefficients of eq.(11) from simulated data.

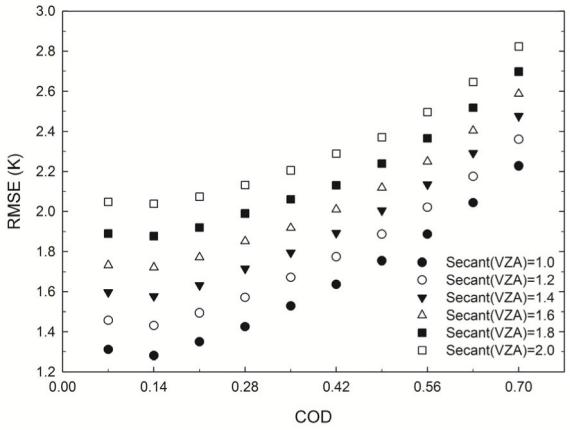

FIGURE 5. RMSEs between the actual LSTs and LST values estimated using eq.(11) versus *COD* for different VZAs in daytime when *R* greater than 20μm.

of the algorithm is also dependent on VZA with the maximum RMSE is 2.8 K when VZA = 60° and COD = 0.7.

B. COMPARISON WITH OTHER ALGORITHM

To estimate the improvement of the proposed algorithm on LST retrieval in cirrus cloudy skies, the LST is recalculated with the generalized split window (GSW) algorithm. It can be expressed as:

$$LST = m_0 + (m_1 + m_2\frac{1-\varepsilon_2}{\varepsilon_2} + m_3\frac{\Delta\varepsilon_2}{\varepsilon_2^2})\frac{T_{31}+T_{32}}{2} + (m_4 + m_5\frac{1-\varepsilon_2}{\varepsilon_2} + m_6\frac{\Delta\varepsilon_2}{\varepsilon_2^2})\frac{T_{31}-T_{32}}{2} \quad (12)$$

where ε_2 is the mean emissivity in channels 31 and 32 and $m_i(i = 0{-}6)$ are the coefficients of the GSW algorithm. Other symbols in Eq.(12) have the same meaning as in Eq.(11). Because the GSW algorithm is one of the most commonly used methods to estimate LST from remotely sensed data and it has been validated by in-situ measurements with RMSE within 1 K under normal clear-sky conditions [13], the result of the three-channel algorithm is compared with the result of GSW algorithm.

To improve the LST retrieval accuracy, the total WVC, LSE and LST for each VZA are divided into several tractable sub-ranges in the GSW algorithm. In this study, we divide the total WVC into five groups with an overlap of 0.5 g/cm^2: 0-1.5, 1.0-2.5, 2.0-3.5, 3.0-4.5 and 4.0-5.0 g/cm^2. Five groups of coefficients m_i ($i = 0 - 6$) in Eq.(12) are then determined for each VZA by using the statistical regression Levenberg-Marquardt method from Dataset-1.

Figure 6. shows the histograms of the differences between LST retrieved employing GSW algorithm using Dataset-2 (include the influence of thin cirrus clouds) and the actual LST when VZA = 0° and VZA = 60°. The RMSE values are 1.89 K and 2.32K for VZA = 0° and VZA = 60° respectively when COD = 0.07; they are 16.89 K and 22.32 K when COD = 0.7. The results of GSW algorithm shows that the clear-sky algorithm is unadaptable for the estimate of LST in cirrus cloudy skies and compared with Figure 5, the proposed algorithm can significantly improve the accuracy of the LST retrieved using thermal infrared data.

Considering the scattering effect of cirrus clouds, the radiation from adjacent pixels around target pixel can also be received by satellite. Thus the thermal inhomogeneity of land surface is needed to take into account for the retrieval of LST in cirrus cloudy skies, compared with SST retrieval algorithm [9]. The Dataset-2 is reproduced with the adjacent pixels' temperature 5 K larger than the target temperature, assuming that the emissivity is constant. Using the coefficients determined with Dataset-2 (adjacent pixels' temperature equivalent to the target temperature) and Eq.(11), the target LST is recalculated with the newly produced TOA

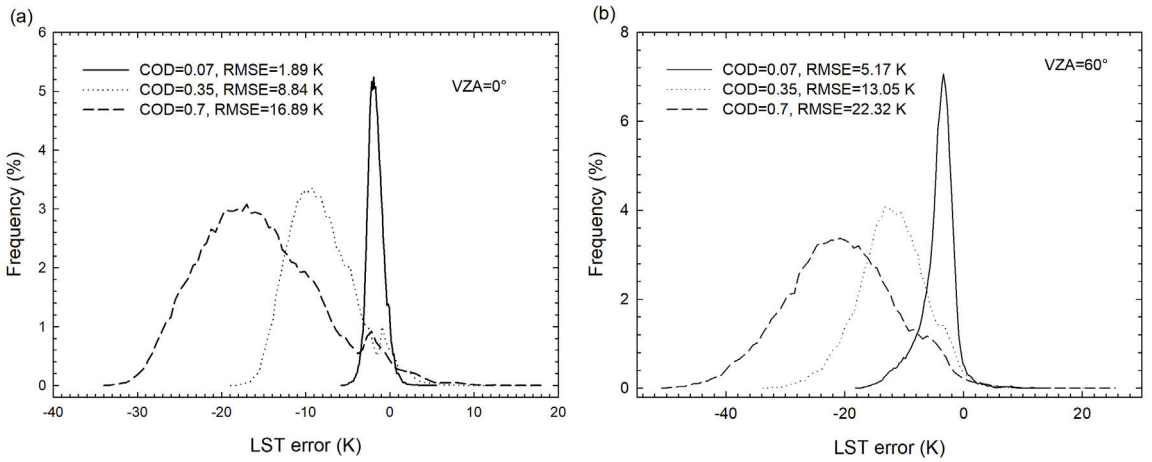

FIGURE 6. Histograms of the differences between the LSTs retrieved employing GSW algorithm using Dataset-2 (include the influence of thin cirrus clouds) and the actual LST when COD = 0.07, 0.35 and 0.7. 6(a) for VZA = 0°, (b) for VZA = 60°.

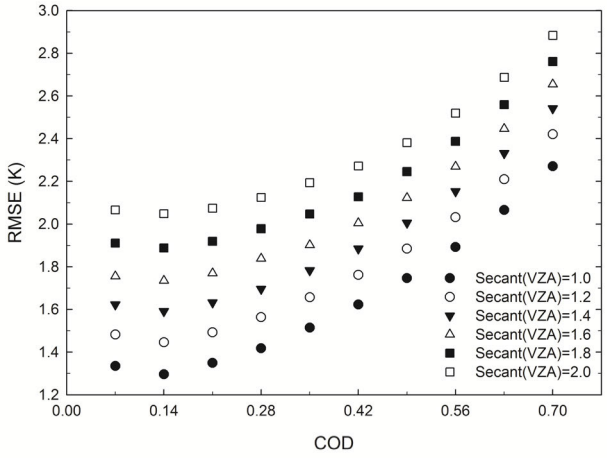

FIGURE 7. RMSEs of LST calculated with eq.(11) employing newly simulated dataset that the adjacent pixels' temperature 5 K larger than the target temperature. The coefficient of eq.(11) is determined with Dataset-2 (adjacent pixels' temperature equivalent to the target temperature).

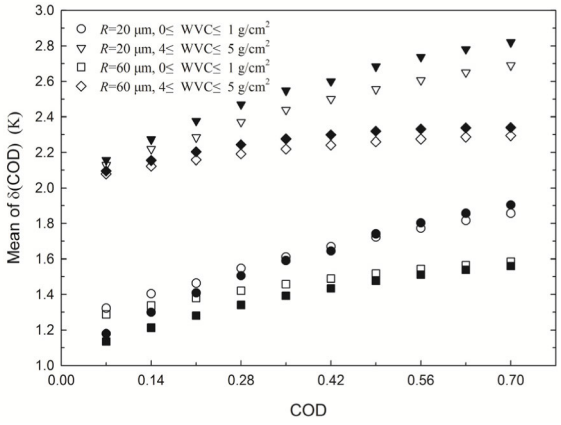

FIGURE 8. Mean values of LST errors δ(COD) caused by the uncertainty of cirrus COD for two different atmospheric WVC range (WVC<1 g/cm^2 and 4 < WVC < 5 g/cm^2) and two different R (R = 20 μm and 60 μm) with VZA = 0° and VZA = 60°, hollow symbols for VZA = 0° and solid symbols for VZA = 60°.

brightness temperatures (adjacent pixels' temperature 5 K larger than the target temperature). The RMSEs between actual target LST and retrieved LST with this newly simulated dataset versus *COD* is shown in Figure 7 for different VZAs.

In Figure 7, the RMSEs become larger compared with Figure 5, but the maximum increasement of RMSE is about 0.07 K when COD is 0.7 and Secant(VZA) = 1.6. It shows that the proposed daytime three-channel LST retrieval algorithm is insensitive to the thermal inhomogeneity of land surface.

V. SENSITIVITY ANALYSIS

The errors in the LST retrieval are affected by many factors, such as the uncertainties of cirrus COD and R, the uncertainty of LSE, the instrument noise and the accuracy of the algorithm itself. Therefore, a sensitivity analysis is performed using the simulated data of Dataset-2 with the following equation:

$$\delta(Y) = LST(X + \Delta(X)) - LST(X), \quad (13)$$

where $\delta(Y)$ is the error of the retrieved LST, X is the value of the sensitivity analysis parameter, $\Delta(X)$ is the error in X, $LST(X + \Delta(X))$ and $LST(X)$ are the retrieved LST values when the parameters are $X + \Delta(X)$ and X, respectively. As an example, only the simulated data with VZAs of 0° and 60° are used in the following sensitivity analysis.

A. SENSITIVITY TO COD

According to Equation (13), the LST errors due to the uncertainty of COD (δ(COD)) can be expressed as:

$$\delta(COD) = \Delta(COD) \left| w_2 * (T_{31} - T_{29}) + w_5 * (T_{31} - T_{32}) + w_{10} \right|, \quad (14)$$

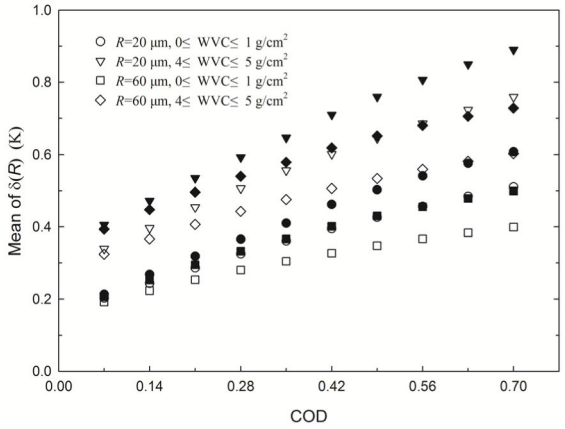

FIGURE 9. Mean values of LST errors $\delta(R)$ caused by the uncertainty of R for two different atmospheric WVC range (WVC$<$1 g/cm^2 and 4 $<$ WVC $<$ 5 g/cm^2) and two different R ($R = 20\ \mu$m and 60 μm) with VZA $= 0°$ and VZA $= 60°$; hollow symbols for VZA $= 0°$and solid symbols for VZA $= 60°$.

where Δ(COD) is the uncertainty of *COD*. To investigate the sensitivity of the proposed algorithm to COD in this analysis, four representative cases are considered, with two different sub-ranges of the atmospheric WVC (WVC $<$ 1 g/cm^2 and 4 $<$ WVC $<$ 5 g/cm^2) and two different R ($R = 20\mu$m and 60 μm) as emissivity values of around 0.99 (land cover type of conifers). Using the simulated TOA brightness temperatures (T_{29}, T_{31} and T_{32}) and assuming Δ(COD) $= 0.1$ in this study, it is possible to calculate δ(COD). Figure 8 shows the mean values of δ(COD) versus COD; hollow symbols for VZA $= 0°$ and solid symbols for VZA $= 60°$.

It shows that the proposed LST retrieval algorithm is more sensitive to COD when wet atmosphere and small cirrus equivalent size conditions. The LST errors are less than 1.9 K in dry atmosphere conditions and the maximum errors are 2.7 K and 2.8 K for VZA $= 0°$ and VZA $= 60°$ respectively when 4$<$ WVC $<$ 5 g/cm^2 and $R = 20\ \mu$m.

B. SENSITIVITY TO R

Similarly, the LST errors due to the uncertainty of R ($\delta(R)$) can be calculated as:

$$\delta(R) = \Delta(R)\left|w_3 * (T_{31} - T_{29}) + w_6 * (T_{31} - T_{32}) + w_{11}\right|, \quad (15)$$

where $\Delta(R)$ is the uncertainty of R. Assuming Δ(R) $= 3\ \mu$m, the mean values of $\delta(R)$ versus COD in four different conditions are shown in Figure 9.

In Figure 9 the mean values of $\delta(R)$ are less than 0.9 K for all the conditions. Similar as the sensitivity of COD, the LST errors caused by R are larger when wet atmosphere and small cirrus equivalent size conditions. Besides that, larger VZA values produce the greater LST errors.

C. SENSITIVITY TO INSTRUMENT NOISE AND LSE

Considering the MODIS noise equivalent temperature difference (NETD) of 0.05 K for channels 29, 31 and 32, the LST errors $\delta(T_{29})$, $\delta(T_{31})$ and $\delta(T_{32})$ caused by instrument noise $\Delta(T_{29})$, $\Delta(T_{31})$ and $\Delta(T_{32})$ are calculated following Eq.(13). Figure 10 gives the mean values of LST errors $\delta(T_{29})$, $\delta(T_{31})$ and $\delta(T_{32})$ versus COD when $R = 20\ \mu$m (hollow symbols) and $R = 60\ \mu$m (solid symbols) for two different VZAs. Figure 10 (a) for VZA $= 0°$ and (b) for VZA $= 60°$.

Figure 10(a) and (b) both illuminate that the newly proposed algorithm is more sensitive to the split window channels 31 and 32, compared with channel 29. It indicates that the split-window channels are more important for the estimate of LST in cirrus conditions. The maximum LST errors caused by instrument noise is 0.4 K when COD is 0.7 and $R = 60\ \mu$m.

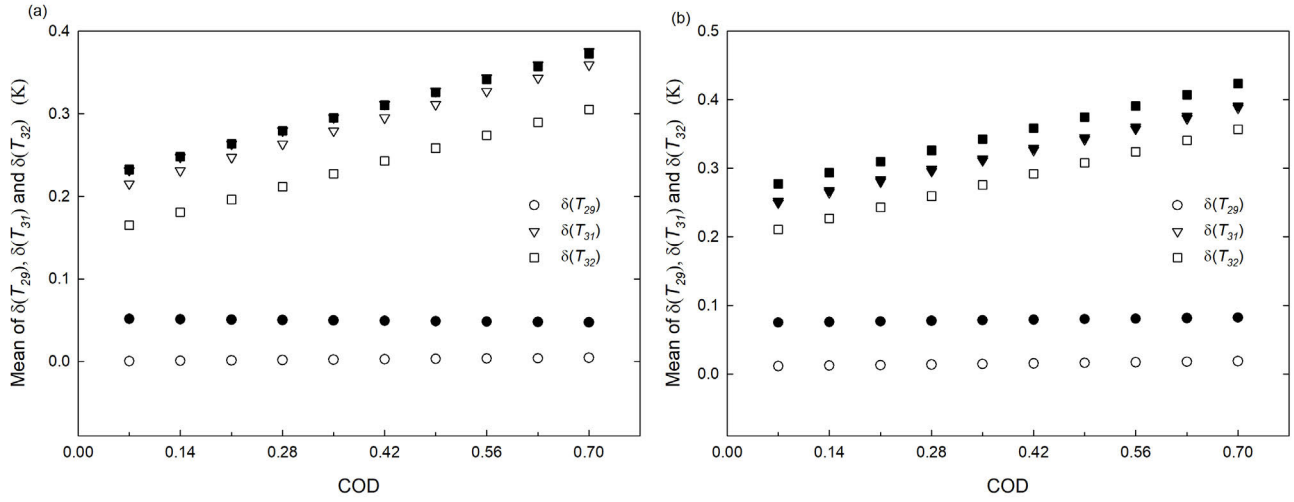

FIGURE 10. Mean values of LST errors $\delta(T_{29})$, $\delta(T_{31})$ and $\delta(T_{32})$ caused by instrument noise $\Delta(T_{29})$, $\Delta(T_{31})$ and $\Delta(T_{32})$ respectively versus COD when $R = 20\ \mu$m (hollow symbols) and $R = 60\mu$m (solid symbols) for two different VZAs. (a) for VZA $= 0°$ and (b) for VZA $= 60°$.

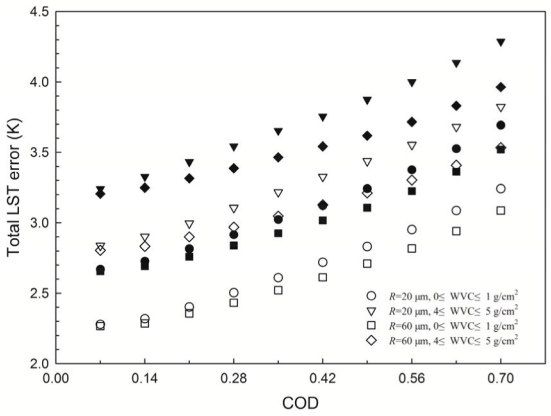

FIGURE 11. Total LST errors associated to the estimation of the LST from the proposed algorithm (Eq. (11)) for four typical situations in two different observation angles. Four typical situations include two atmospheric WVC ranges (WVC < 1 g/cm^2 and 4 < WVC < 5 g/cm^2) and two R conditions. Hollow symbols for VZA = 0°and solid symbols for VZA = 60°.

Assuming the uncertainties in $\Delta\varepsilon_1$, ε_1 and $\Delta\varepsilon_2$ are 0.01, the LST errors due to the LSE errors are 0.11 K, 0.42 K and 1.19 K respectively when VZA = 0°; those errors are 0.03 K, 0.37 K and 1.12 K respectively when VZA = 60°. The analysis indicates that the emissivity difference in split-window channels is more important for the accuracy of the proposed algorithm with the LST errors from $\Delta\varepsilon_2$ nearly 1 K.

D. TOTAL LST ERRORS

To study the total LST errors caused by all the input parameters' uncertainties and the algorithm error itself, the $\delta(LST_{total})$ has been calculated according to the expression $\delta\,(LST_{total}) = \sqrt{\delta^2_{minimization} + \delta^2_{theory}}$, where $\delta_{minimization}$ is the accuracy of the algorithm itself and

$$\delta_{theory} = \sqrt{\begin{array}{l}\delta\,(COD)^2 + \delta\,(R)^2 + \delta\,(T_{29})^2 + \delta\,(T_{31})^2 \\ +\delta\,(T_{32})^2 + \delta\,(\Delta\varepsilon_1)^2 + \delta\,(\varepsilon_1)^2 + \delta\,(\Delta\varepsilon_2)^2\end{array}}, \tag{16}$$

The total LST errors in four typical situations versus COD are given in Figure 11. Hollow symbols are VZA = 0° and solid symbols are VZA = 60°. It shows that the dry atmospheric conditions with greater cirrus size produce the smaller total LST errors. The total errors increase with COD and the maximum error is 4.3 K when COD = 0.7, R = 20 μm, VZA = 60° and wet atmospheres. Because the errors from different variables can be neutralized, the actual values are usually smaller than the estimated values. From the analysis above, to obtain an accurate LST in cirrus cloudy skies, the better quality of COD is important.

VI. CONCLUSION

To estimate daytime land surface temperatures (LSTs) in thin cirrus cloudy skies, we have proposed a three-channel algorithm based on a widely used two-channel LST retrieval algorithm for clear-sky conditions. Using a couple of two-channel algorithms in three different channels, the LST is expressed as a multiple linear function of top of the atmosphere (TOA) brightness temperature in MODIS channel 31, difference between channels 31 and 29, difference between channels 31 and 32. The simulated dataset shows that the LST could be estimated using the proposed three-channel algorithm with the root mean squire error (RMSE) less than 2.2 K in thin cirrus cloudy skies (COD less than 0.7) when viewing zenith angle (VZA) equivalent to 0°. As VZA is equivalent to 60°, the maximum RMSE is 2.7 K.

The widely used generalized split-window (GSW) algorithm proposed for clear-sky conditions are used in cirrus cloudy skies, and the RMSEs of GSW algorithm estimated LST are 16.89 K and 22.32 K for VZA = 0° and VZA = 60° respectively when COD is 0.7. It indicates that the proposed three-channel algorithm can significantly improve the LST retrieval accuracy in cirrus cloudy skies. Because of the scattering effect of cirrus clouds, the influence of land surface inhomogeneity is analyzed in this study. With the simulated data that the adjacent pixels' temperature 5 K larger than the target temperature, there is no obvious degradation of the accuracy of the three-channel algorithm with the RMSEs increase at most 0.07 K. It shows that this algorithm is insensitive to the uncertainty of land surface inhomogeneity.

In addition, a sensitivity analysis of the algorithm was performed to assess the LST errors in terms of cirrus COD, R, LSE, instrument noise and algorithm error itself. It shows that the accuracy of cirrus COD is more important to get a reliable estimate of LST compared with R, LSE and instrument noise, with LST errors from COD as much as 1.9 K. When all the uncertainties of input parameters and algorithm errors are taken into account, the maximum total LST error are 3.8 K and 4.3 K when VZA = 0° and VZA = 60° respectively. Because of the shortage of field measured MODIS pixel scale LSTs in cirrus cloudy skies, we only used the simulated data in this study. It should be pointed out that the proposed three-channel LST retrieval algorithm certainly needs to be validated using field measurement in the further work. As the clouds' parameters of R and COD are used, the proposed algorithm can only be used for the day-time when R and COD are available. In addition, this study focus on LST retrieval under cirrus clouds, the LST retrieval algorithm for different cloud types need to be studied in the future work.

REFERENCES

[1] J. U. Duncombe, "Infrared navigation—Part I: An assessment of feasibility," *IEEE Trans. Electron Devices*, vol. ED-11, no. 1, pp. 34–39, Jan. 1959.
[2] Z.-L. Li, R. Tang, Z. Wan, Y. Bi, C. Zhou, B. Tang, G. Yan, and X. Zhang, "A review of current methodologies for regional evapotranspiration estimation from remotely sensed data," *Sensors*, vol. 9, no. 5, pp. 3801–3853, May 2009.
[3] Z.-L. Li, B.-H. Tang, H. Wu, H. Ren, G. Yan, Z. Wan, I. F. Trigo, and J. A. Sobrino, "Satellite-derived land surface temperature: Current status and perspectives," *Remote Sens. Environ.*, vol. 131, pp. 14–37, Apr. 2013.
[4] F. Becker and Z.-L. Li, "Towards a local split window method over land surfaces," *Int. J. Remote Sens.*, vol. 11, no. 3, pp. 369–393, Mar. 1990.
[5] C. Coll, V. Caselles, E. Valor, and R. Niclòs, "Comparison between different sources of atmospheric profiles for land surface temperature retrieval from single channel thermal infrared data," *Remote Sens. Environ.*, vol. 117, pp. 199–210, Feb. 2012.

[6] D. K. Lynch, K. Sassen, D. O. C. Starr, and G. Stephens, "Cirrus: History and definitions," in *Cirrus*. New York, NY, USA: Oxford Univ. Press, 2002, pp. 3–10.
[7] L. Xu and B. Sun, "Influence of cirrus clouds on the VISSR atmospheric sounder-derived sea surface temperature determinations," *Appl. Opt.*, vol. 30, no. 12, pp. 1525–1536, 1991.
[8] W. L. Smith, S. Ackerman, H. Revercomb, H. Huang, D. H. DeSlover, W. Feltz, L. Gumley, and A. Collard, "Infrared spectral absorption of nearly invisible cirrus clouds," *Geophys. Res. Lett.*, vol. 25, no. 8, pp. 1137–1140, Apr. 1998.
[9] L. Xu, J. Zhang, G. Zhang, and H. Chen, "Simulation of remote sensing of sea surface temperature from space: Influences of cirrus clouds and stratospheric aerosols on sea surface temperatures derived from the VISSR atmospheric sounder," *Int. J. Remote Sens.*, vol. 15, no. 13, pp. 2599–2614, Sep. 1994.
[10] X. Fan, B.-H. Tang, H. Wu, G. Yan, and Z.-L. Li, "A three-channel algorithm for retrieving night-time land surface temperature from MODIS data under thin cirrus clouds," *Int. J. Remote Sens.*, vol. 36, nos. 19–20, pp. 4836–4863, Oct. 2015.
[11] X. Fan, B.-H. Tang, H. Wu, G. Yan, and Z.-L. Li, "Daytime land surface temperature extraction from MODIS thermal infrared data under cirrus clouds," *Sensors*, vol. 15, no. 5, pp. 9942–9961, Apr. 2015.
[12] F. Parol, J. C. Buriez, G. Brogniez, and Y. Fouquart, "Information content of AVHRR channels 4 and 5 with respect to the effective radius of cirrus cloud particles," *J. Appl. Meteorol.*, vol. 30, no. 7, pp. 973–984, Jul. 1991.
[13] Z. Wan, "New refinements and validation of the MODIS land-surface temperature/emissivity products," *Remote Sens. Environ.*, vol. 112, no. 1, pp. 59–74, Jan. 2008.
[14] G. P. Berk, L. S. Anderson, P. K. Bernstein, H. Acharya, M. Dothe, W. Matthew, S. M. Adler-Golden, J. H. Chetwynd, S. C. Richtsmeier, B. Pukall, C. L. Allred, L. S. Jeong, and M. L. Hoke, "MODTRAN4 radiative transfer modeling for atmospheric correction," *Proc. SPIE.*, vol. 3756, pp. 348–353, Oct. 1999.
[15] J. M. Galve, C. Coll, V. Caselles, and E. Valor, "An atmospheric radiosounding database for generating land surface temperature algorithms," *IEEE Trans. Geosci. Remote Sens.*, vol. 46, no. 5, pp. 1547–1557, May 2008.
[16] H. Wu, L. Ni, N. Wang, Y. Qian, B.-H. Tang, and Z.-L. Li, "Estimation of atmospheric profiles from hyperspectral infrared IASI sensor," *IEEE J. Sel. Topics Appl. Earth Observ. Remote Sens.*, vol. 6, no. 3, pp. 1485–1494, Jun. 2013.
[17] A. M. Baldridge, S. J. Hook, C. I. Grove, and G. Rivera, "The ASTER spectral library version 2.0," *Remote Sens. Environ.*, vol. 113, no. 4, pp. 711–715, Apr. 2009.
[18] B. A. Baum, P. Yang, A. J. Heymsfield, A. Bansemer, B. H. Cole, A. Merrelli, C. Schmitt, and C. Wang, "Ice cloud single-scattering property models with the full phase matrix at wavelengths from 0.2 to 100 μm," *J. Quant. Spectrosc. Radiat. Transf.*, vol. 146, pp. 123–139, Oct. 2014.
[19] B. A. Baum, P. Yang, A. J. Heymsfield, S. Platnick, M. D. King, Y.-X. Hu, and S. T. Bedka, "Bulk scattering properties for the remote sensing of ice clouds. Part II: Narrowband models," *J. Appl. Meteorol.*, vol. 44, no. 12, pp. 1896–1911, Dec. 2005.
[20] D. R. Dowling and L. F. Radke, "A summary of the physical properties of cirrus clouds," *J. Appl. Meteorol.*, vol. 29, no. 9, pp. 970–978, Sep. 1990.
[21] B. Tang, Y. Bi, Z.-L. Li, and J. Xia, "Generalized split-window algorithm for estimate of land surface temperature from Chinese geostationary FengYun meteorological satellite (FY-2C) data," *Sensors*, vol. 8, no. 2, pp. 933–951, Feb. 2008.
[22] J. A. Sobrino and N. Raissouni, "Toward remote sensing methods for land cover dynamic monitoring: Application to Morocco," *Int. J. Remote Sens.*, vol. 21, no. 2, pp. 353–366, Jan. 2000.
[23] K. N. Liou, *Radiation and Cloud Process in the Atmosphere: Theory, Observation and Modeling*. New York, NY, USA: Oxford Univ. Press, 1992, pp. 186–188.
[24] J. Sobrino, C. Coll, and V. Caselles, "Atmospheric correction for land surface temperature using NOAA-11 AVHRR channels 4 and 5," *Remote Sens. Environ.*, vol. 38, no. 1, pp. 19–34, Oct. 1991.
[25] J. A. Sobrino, Z.-L. Li, M. P. Stoll, and F. Becker, "Multi-channel and multi-angle algorithms for estimating sea and land surface temperature with ATSR data," *Int. J. Remote Sens.*, vol. 17, no. 11, pp. 2089–2114, Jul. 1996.
[26] H. Nazaryan, M. P. McCormick, and W. P. Menzel, "Global characterization of cirrus clouds using CALIPSO data," *J. Geophys. Res.*, vol. 113, no. D16, p. 211, 2008.

XIWEI FAN received the Ph.D. degree in cartography and geographical information system from the Institute of Geographic Sciences and Natural Resources Research, Chinese Academy of Sciences, Beijing, in 2015. He is currently an Associate Research Fellow with the Institute of Geology, China Earthquake Administration. His research interests include the retrieval and validation of land surface temperature/emissivity and earthquake damage estimation.

GAOZHONG NIE received the Ph.D. degree in quaternary geology from the Institute of Geology, Chinese Academy of Sciences, Beijing, China, in 1990. He is currently a Researcher with the Institute of Geology, China Earthquake Administration. His research interests include the earthquake disaster risk assessment and land surface temperature retrieval.

YAOHUI LIU received the Ph.D. degree in quaternary geology from the Institute of Geology, China Earthquake Administration, China, in 2020. He is currently a Lecturer with Shandong Jianzhu University. His research interests include computer vision, remote sensing, deep learning, and risk management.

LI NI received the Ph.D. degree in cartography and geographical information system from the Institute of Remote Sensing and Digital Earth, Chinese Academy of Sciences, Beijing, China, in 2015. She is currently an Associate Researcher with the Aerospace Information Research Institute, Chinese Academy of Sciences. Her research interests include the land surface temperature retrieval and application of hyperspectral remote sensing.